Original articles

Research article
https://doi.org/10.17308/kcmf.2022.24/10560

Growth kinetics of anodic oxide layers on cobalt silicides in sulphuric acid solutions

A. B. Shein✉, V. I. Kichigin

*Perm State National Research University,
15 Bukireva ul., Perm 614990, Russian Federation*

Abstract

The aim of this research was to study the growth kinetics of anodic oxide films on cobalt silicides in sulphuric acid solutions under potentiostatic conditions with various pretreatment of the electrode surface. For the study, we used low and high silicon silicides (Co_2Si and $CoSi_2$) in 0.05 and 0.5 M H_2SO_4.

We obtained the chronoamperograms in the time interval t = 0.3–3000 s with the oxide formation potentials of E_f = 0.2, 0.5, and 1.0 V (SHE). It was determined that the kinetics of the growth of oxide layers on cobalt silicides in acidic solutions greatly depends on the method of the silicide surface pretreatment (mechanical polishing; cathodic pre-polarisation in a H_2SO_4 solution; exposure to H_2SO_4 solution at the open circuit potential; exposure in a 2 M KOH solution; and exposure to 2% HF solution). In most cases, at low t (up to 30–50 s), the oxide films grew due to the ion migration in the strong electric field generated in the film during anodic polarisation.

In some cases (Co_2Si silicide with higher cobalt content; pretreatment of Co_2Si in alkaline solution, further enriching the silicide surface with cobalt; and the region of high values of t), the point defect model seemed to be executed.

Keywords: Cobalt silicide, Passivity, Oxide film, Growth kinetics, High field model, Point defect model

For citation: Shein A. B., Kichigin V. I. Growth kinetics of anodic oxide layers on cobalt silicides in sulphuric acid solutions. *Condensed Matter and Interphases.* 2022;24(4): 559–571. https://doi.org/10.17308/kcmf.2022.24/10560

Для цитирования: Шеин А.Б., Кичигин В.И. Кинетика роста анодных оксидных слоев на силицидах кобальта в растворах серной кислоты. *Конденсированные среды и межфазные границы.* 2022;24(4): 559–571. https://doi.org/10.17308/kcmf.2022.24/10560

✉ Anatoly B. Shein, e-mail: ashein@psu.ru

1. Introduction

One of the most important characteristics of the corrosion and electrochemical behaviour of metals and alloys is the tendency for anodic passivation [1]. The passivity phenomenon is of great practical importance, because the formation of the passivating oxide films makes many materials highly resistant to corrosion in media where oxide layers are difficult to dissolve. In this regard, various aspects of anodic passivity are extensively studied, including the kinetics of the nucleation and growth of anodic oxide films (AOF).

The high corrosion resistance of transition metal silicides [2–10] is also attributed to the formation of dense passive films. The composition of oxide films on the transition metal silicides depends primarily on the silicide composition [5], the electrode potential [3], and pH of the solution [3]. When the silicon content in the silicide increases, the composition of the oxide film approaches that of SiO_2 [3, 4, and 11]. According to [12], on Fe-Si alloys (at ⩾ 21 at.% of Si), the outer part of the oxide film in a solution at pH 9 contains only Fe, and at pH 5 it contains about 50 at.% of Fe. In other words, the Fe content in the oxide layer decreases as the pH decreases. In strongly acidic solutions, almost pure protective SiO_2 is formed and Fe is dissolved.

In research [13], the results of the study of anodic oxide layers on FeSi, CoSi, and NiSi monosilicides in a 0.5 M H_2SO_4 solution were presented. Linear dependences of the layer thickness on the electrode potential E in the range of 0.5–1.1 V (SHE) were obtained. The calculated values of the specific electrical resistance of the oxide films demonstrated that the anodic oxide may contain small amounts of metal. Cyclic voltammetry showed that after the initiation of anodic polarisation, the metal atoms preferentially dissolved, i.e., silicon accumulated on the electrode surface. This is a precondition for the formation of oxide films with high barrier properties.

The growth patterns of the AOF on alloys are more complex than on pure metals [14–18]. This also applies to metal-silicon alloys. While some data on the composition of oxide films on transition metal silicides is available, the kinetics of the AOF growth on these materials has not been studied. The purpose of this research was to study the kinetics of the formation of anodic oxides on Co_2Si and $CoSi_2$ cobalt silicides in sulphuric acid solutions under potentiostatic conditions upon different pretreatment of the electrode surface.

2. Experimental

In this study, we used Co_2Si and $CoSi_2$ cobalt silicides obtained by the Czochralski method. To study the AOF growth, the electrode surface must be unoxidised before the potential step is applied [19]. Therefore, we used various methods to ensure an active surface at the beginning of the experiment by removing the oxides formed due to the contact of the silicide with the air. When choosing these methods, we took into account possible chemical processes involving cobalt and silicon oxides, which may occur on the silicide surface. Differences in the state of the surface of the silicides resulting from different pretreatment methods are evident at the nucleation stage of the oxide phase, when the anode potential is applied. They affect the growth of the AOF and, consequently, the anodic current as a function of time.

The following electrode surface pretreatment methods were used:

1) Polishing with abrasive paper (finishing by P4000 paper), cleaning with ethyl alcohol, and rinsing in the working solution. Mechanical surface conditioning also preceded the other pretreatment methods.

2) Cathodic activation (1 mA/cm², 20 min). Cathodic oxide reduction is often used (e.g., [14, 20]) to remove oxide films from the electrode surface. We also used this method. Though, in the case of cobalt silicides, cathodic activation may be ineffective, because anodic oxide films on Co_2Si are hard to reduce. On $CoSi_2$, cathodic reduction of anodic oxides barely takes place [21].

3) Exposure to 0.5 M H_2SO_4 at an open circuit potential, $E_{oc,}$ for 30 min. This treatment has almost no effect on the silica component of the oxide, but can affect cobalt oxides.

4) Exposure to 2% HF at E_{oc} for 5 min, rinsing in deionised water and in working solution. HF is known to dissolve SiO_2 effectively [22], but it has almost no effect on silicon (it may dissolve one monolayer of silicon atoms) [23]. A 2% HF solution can also remove the cobalt component

of the oxide. This type of pretreatment probably provides the most oxide-free electrode surface.

As a variation of this pretreatment, we also used a 10 min exposure to 0.5 M H_2SO_4 + 0.05 M HF at E_{oc}. It was assumed that HF would dissolve SiO_2 and the presence of sulphuric acid would lead to a faster dissolution of the cobalt oxides.

5) Exposure in 2 M KOH at E_{oc} for 40 min, rinsing (neutralisation) in the working solution, and transfer to the electrochemical cell with or without the electrode exposure at E_{oc}. In alkaline solutions, both silicon and silicon oxide dissolve [24], the silicide surface is enriched with a metallic component [2]. The exposure time was chosen in view of the results obtained in [25]. The study showed that the self-activation of Co_2Si electrode in 2 M KOH occurs in about 2000 s (~33 min). The treatment in a KOH solution does not affect the cobalt oxides (if they are present in the oxide film). The cobalt oxide may partially dissolve after transferring the electrode to a cell with a sulphuric acid solution.

The measurements were carried out at room temperature (22–25 °C) in non-deaerated solutions of 0.5 M H_2SO_4 and 0.05 M H_2SO_4 prepared from a chemically pure reagent and deionised water (Millipore). We used the following measurement procedure: the potential was changed from E_{oc} of the electrode, pretreated by one of the above methods, to a given value of E_f (in the range of 0.2–1.0 V, all potentials are provided for standard hydrogen electrode) for 50 minutes. The I,t curve (I is the current, t is the time) was recorded. The E_{oc} values for each of the silicides varied only slightly depending on the electrode pretreatment method (Tables 1, 2). Therefore, the value of $E_f – E_{oc}$ at a given E_f was also approximately the same for different

Table 1. The values of $d\lg i/d\lg t$ for Co_2Si passivation in H_2SO_4 solutions

Pretreatment of electrode surface	Concentration of H_2SO_4, M	E_{oc}, V	E_f, V	$d\lg i/d\lg t$	Time interval, s
Mechanical polishing	0.05	−0.266	0.5	−0.86	< 200
Mechanical polishing	0.05	−0.266	1.0	−0.80	< 200
Mechanical polishing	0.5	−0.232	0.5	−0.61 −0.92	1–10 50–2000
Mechanical polishing	0.5	−0.232	1.0	−0.70	< 10
30 min in 0.5 M H_2SO_4 at E_{oc}	0.5	−0.225	1.0	−1.0 −0.84	5–30 100–3000
Cathodic polarization	0.5	−0.233	1.0	−0.71 −0.94	< 10 30–1000
Treatment in 2% HF	0.05	−0.270	1.0	−0.94 −0.86	1–10 500–1000
Treatment in 2% HF	0.5	−0.235	0.2	−0.76 −0.85	1–100 200–1000
Treatment in 2% HF	0.5	−0.235	0.5	−0.65 −1.2	1–30 500–3000
Treatment in 2% HF	0.5	−0.235	1.0	−0.78 −1.4	0.3–20 > 1250
Treatment in 0.5 M H_2SO_4 + 0.05 M HF, 10 min	0.5	−0.233	0.5	-0.77	5–100
Treatment in 0.5 M H_2SO_4 + 0.05 M HF, 10 min	0.5	−0.235	1.0	-0.87	1–220
Treatment in 2 M KOH	0.05	−0.278	1.0	−0.57 −0.91	3–15 30–1000
Treatment in 2 M KOH	0.5	−0.223	0.5	−0.66	1–10
Treatment in 2 M KOH	0.5	−0.223	1.0	−0.64 −0.84	< 2 30–1000
Treatment in 2 M KOH, 30 min in 0.5 M H_2SO_4 at E_{oc}	0.5	−0.21	1.0	−0.77 −0.89	< 2 10–1000

Table 2. The values of $d \lg i/d \lg t$ for $CoSi_2$ passivation in H_2SO_4 solutions

| Pretreatment of electrode surface	Concentration of H_2SO_4, M	E_{oc}, V	E_f, V	$d \lg i/d \lg t$	Time interval, s
Mechanical polishing	0.5	+0.12	1.0	−0.87	2–20
Treatment in 2 M KOH	0.5	−0.09	1.0	−0.67 −0.78 −0.84	< 10 10–100 100–1000
Treatment in 2 M KOH	0.5	−0.09	0.5	−0.64 −0.86	1–10 100–1000
Treatment in 2% HF	0.5	−0.10	1.0	−0.83 −1.4	< 10 200–450
Treatment in 2% HF	0.5	−0.10	0.5	−0.72 −0.98	< 10 200–500
Treatment in 2% HF	0.5	−0.10	0.2	−0.50 −1.0	10–50 200–1000
Treatment in 2% HF	0.05	−0.145	1.0	−0.88 −0.71 −1.1	1–5 60–200 300–1000

types of surface treatment. The measurements were taken with a Solartron 1287 potentiostat (Solartron Analytical). The data collection rate was 5 points per second.

3. Results and discussion

In some cases, the $\lg i, \lg t$ dependences had a simple form of a single linear section (with a negative slope slightly less than 1) with the current density reaching a steady-state value at high t (Fig. 1). However, in most cases, chronoamperograms had a more complex shape with several linear sections, inflection points, etc. (Fig. 2). The values of the $d \lg i/d \lg t$ slopes for the Co_2Si electrode are provided in Table 1.

Preliminary cathodic polarisation of the Co_2Si electrode in 0.5 M H_2SO_4 had very little effect on the i,t-curves (Fig. 2). The current density slightly increased, while the shape of $\lg i, \lg t$-dependence did not change. Pre-exposure of the electrode in a 2 M KOH solution had a more prominent effect (Fig. 2). At short passivation time (up to $t \sim 50$ s), the shapes of the $\lg i, \lg t$-curves depend on the pretreatment of the electrode surface. The lowest values of the current density were observed when the electrode was washed in deionised water and transferred to the measuring cell after exposure in a KOH solution. Higher current densities were observed when the electrode was washed in a 0.5 M H_2SO_4 solution after exposure in a KOH solution (in this case, the alkaline solution remaining on the electrode was quickly neutralised) and then

transferred to the measuring cell. Even higher current densities were observed when, after exposure to a KOH solution and neutralisation in 0.5 M H_2SO_4, the electrode was kept for 30 min at the open circuit potential in a cell with a working solution of 0.5 M H_2SO_4. The increase in i at low t in the latter case was probably not
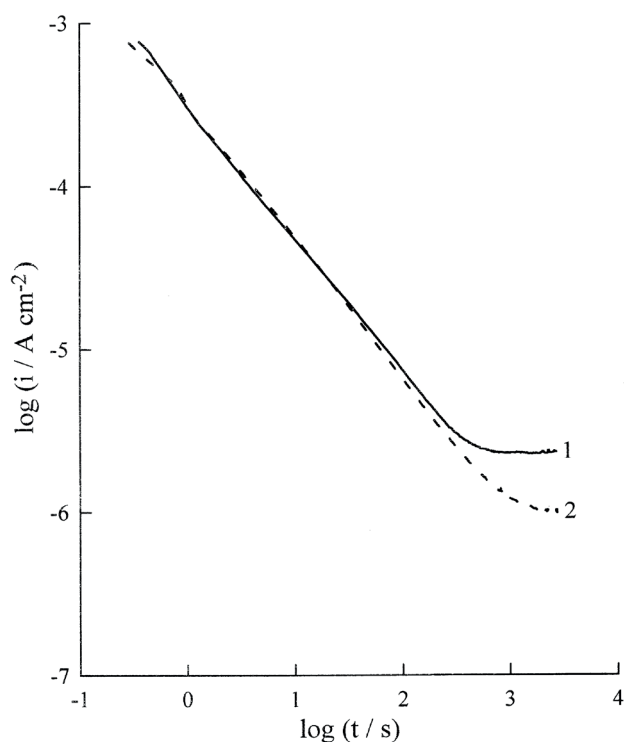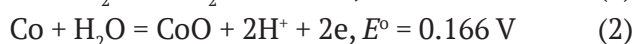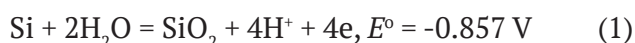

Fig. 1. Chronoamperograms of the Co_2Si electrode in 0.05 M H_2SO_4. *1* – E_f = 1.0 V, *2* – E_f = 0.5 V. Pretreated by mechanical polishing

due to an increase in the true surface area (since at large values of t, the current densities were approximately the same both with exposure at E_{oc} and without it), but to a more complete dissolution of cobalt oxides on the electrode surface due to its exposure at E_{oc}. Exposure of the Co_2Si electrode at the open circuit potential to the working solution without pretreatment in a KOH solution resulted in lower current densities.
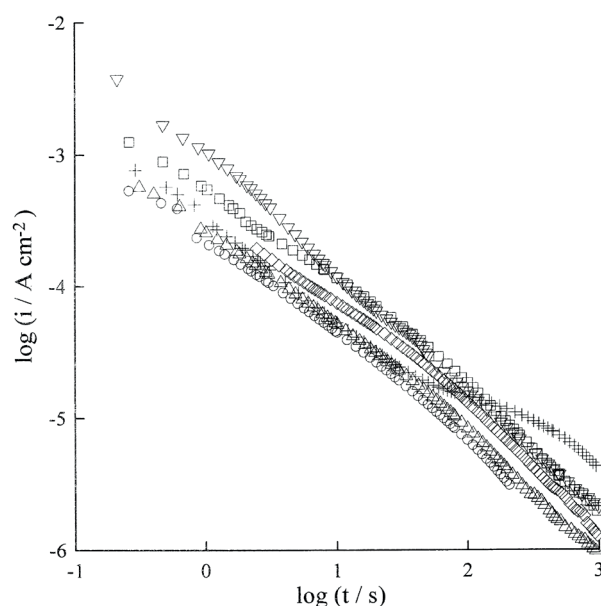
The chronoamperograms for the $CoSi_2$ electrode in logarithmic scale were also similar to the linear dependences (Fig. 3). As in the case of Co_2Si, lower current densities were observed for the electrode with mechanically polished surface. The values of the $d \lg i/d \lg t$ slopes for $CoSi_2$ are provided in Table 2. At the same pretreatment of the electrode, the values of $d \lg i/d \lg t$ for $CoSi_2$ were slightly greater than for Co_2Si (at least at low t).

A characteristic feature of the passivation of cobalt silicides is an inflection on the $\lg i, \lg t$-curve at $t = 30–100$ s, when the surface was pretreated with 2% HF (Fig.4, 5). The inflection was less prominent for the $CoSi_2$ electrode than for the Co_2Si electrode. Upon the transition from Co_2Si to $CoSi_2$, the value of t_{ip} decreased noticeably, while i_{ip} changed less (t_{ip} and i_{ip} are the coordinates of the inflection point). The inflection section became longer with an increase in E_f. In the case of $CoSi_2$, the influence of E_f on the inflection point coordinates was more pronounced than in the case of Co_2Si. When the concentration of sulphuric acid decreased at the same E_f, the value of t_{ip} decreased slightly, and i_{ip} increased. The values of t_{ip} and i_{ip} are provided in Table 3. After the inflection, the $d \lg i/d \lg t$ slope becomes steeper.

The formation of oxide films on cobalt silicides can be associated with the following overall reactions (in the studied potential range up to 1 V)

$$Si + 2H_2O = SiO_2 + 4H^+ + 4e, E^o = -0.857 \text{ V} \qquad (1)$$

$$Co + H_2O = CoO + 2H^+ + 2e, E^o = 0.166 \text{ V} \qquad (2)$$

$$3CoO + H_2O = Co_3O_4 + 2H^+ + 2e, E^o = 0.777 \text{ V} \quad (3)$$

The standard potentials for the reactions were taken from [26]. Reactions (1) and (2) directly describe the oxidation of silicide components, while reaction (3) describes a possible transformation in cobalt oxide.

Fig. 2. Chronoamperograms of the Co_2Si electrode in 0.5 M H_2SO_4 at $E_f = 1.0$ V for different types of the electrode surface pretreatment: ($\bigcirc$) – mechanical polishing; ($\triangle$) – cathodic pre-polarisation of the electrode; ($\diamond$) – exposure of the electrode to 2 M KOH, washing in the deionised water; ($\square$) – exposure of the electrode to 2 M KOH, washing (neutralisation) in 0.5 M H_2SO_4; ($\triangledown$) – exposure of the electrode to 2 M KOH, washing (neutralisation) in 0.5 M H_2SO_4, exposure to 0.5 M H_2SO_4 for 30 min at E_{oc}; and ($+$) – etching in 2% HF
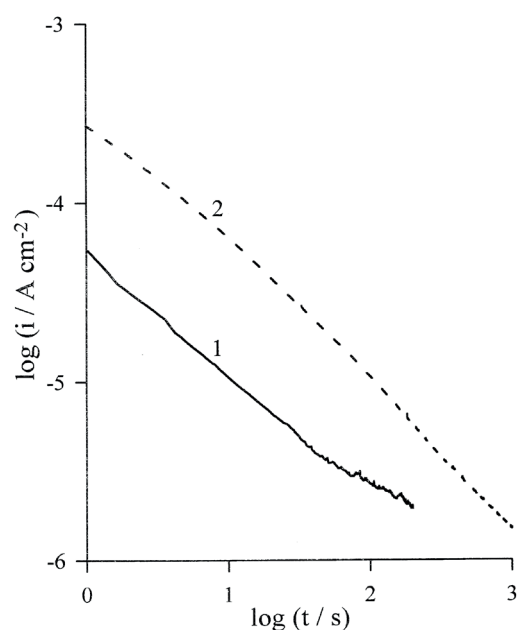
Fig. 3. Chronoamperograms of the $CoSi_2$ electrode in 0.5 M H_2SO_4 at $E_f = 1.0$ V. *1* – mechanical polishing; *2* – exposure to 2 M KOH for 45 min
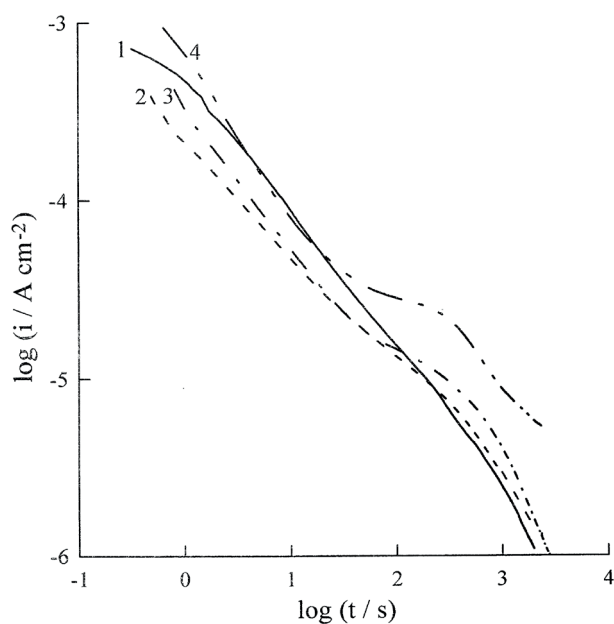
Fig. 4. Chronoamperograms of the Co₂Si electrode in 0.5 M H₂SO₄ (*1–3*) or 0.05 M H₂SO₄ (*4*). The surface was pretreated in 2% HF. Potential E_f, V: *1* – 0.2; *2* – 0.5; and *3, 4* – 1.0
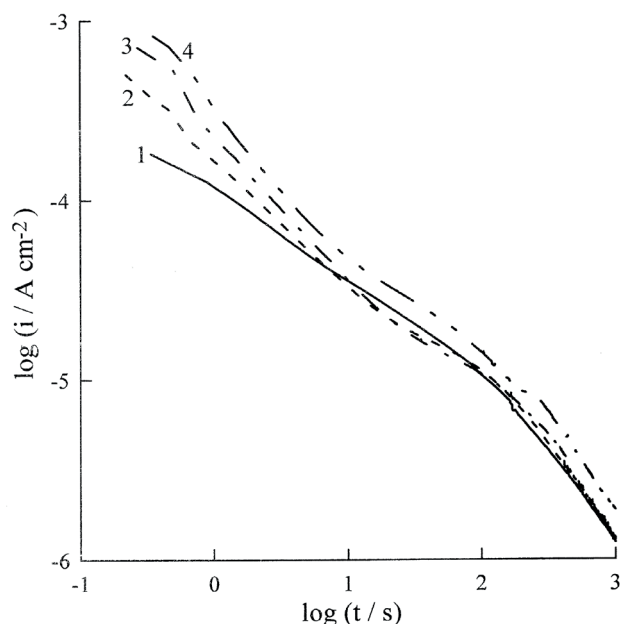
Fig. 5. Chronoamperograms of the CoSi₂ electrode in 0.5 M H₂SO₄ (*1–3*) or 0.05 M H₂SO₄ (*4*). The surface was pretreated in 2% HF. Potential E_f, V: *1* – 0.2; *2* – 0.5; *3, 4* – 1.0

Table 3. Inflection point coordinates (pretreatment with 2% HF)

Silicide	$C_{H_2SO_4}$, M	E_f, V	$\lg t_\text{п}$	$\lg i_\text{п}$
Co₂Si	0.05	1.0	1.95	−4.53
	0.5	0.2	1.93	−4.73
	0.5	0.5	1.94	−4.73
	0.5	1.0	2.03	−4.83
CoSi₂	0.05	1.0	1.39	−4.50
	0.5	0.2	1.34	−4.62
	0.5	0.5	1.63	−4.80
	0.5	1.0	1.74	−4.87

To describe the kinetics of anodic passivation, different models were proposed: the high electric field model [27, 28], point defect model [20, 29–31], generalised oxide growth model [32], and mass-charge balance model [33]. The brief review of the models is provided in [32, 34]. The high field model (HFM) and the point defect model (PDM) can be considered as the key models of the AOF growth, they have been tested on a large number of systems.

The high electric field model describes the movement of ions through interstitial positions in an oxide film by a thermally activated hopping mechanism. Due to this mechanism, a moving ion crosses a certain potential barrier that depends on the electric field in the film. According to the HFM, the rate-determining stage of the oxide film growth is the migration of ions in the oxide or the injection of cations into the oxide at the metal/oxide interface. According to the model, the electric field strength during the oxide growth is very high (> 1 MV/cm). The film growth results in a decrease of the electric field strength in the film (under potentiostatic conditions), and hence in a decrease of the anodic current density. The HFM leads to the approximate fulfilment of the logarithmic growth law or the inverse logarithmic law [27].

According to the point defect model, the ion current in the AOF is carried by nonequilibrium anion and cation vacancies which are generated at the metal/oxide and oxide/electrolyte interfaces. The value of the electric field in the oxide film can be much lower than that in the HFM [28]. It is assumed that the electric field is independent (or little dependent) on the film thickness and electrode potential (this is the main difference between the PDM and HFM). The model takes into account the potential drops at the metal/film $\varphi_\text{m/f}$ and film/solution $\varphi_\text{f/s}$ interfaces, and $\varphi_\text{f/s}$ is the linear function of the applied potential and the pH of the solution. It also takes into account the chemical dissolution of the oxide. The PDM

provides a logarithmic law of the oxide layer growth.

To distinguish between the mechanisms determining the passivation kinetics of silicides, the diagnostic criteria proposed in [20] can be used. When the current densities $i(t)$ are much higher than the steady-state current density, the dependence of $F(i) = (-i')^{1/2}/i$ on $\ln i$ is plotted, where $i' = di/dt$ is the derivative of the current density with respect to time. If the value of $(-i')^{1/2}/i$ is constant, the data are consistent with the point defect model. If $(-i')^{1/2}/i$ increases linearly with $\ln i$, the high field model of film growth is applicable. When the current densities become comparable with the steady-state current density i_s, the dependence of $[-i'/i(i - i_s)]^{1/2}$ on $\ln i$ should be considered [20].

The theoretical expression for $(-i')^{1/2}/i$ in the case of the high electric field model is presented as [20]:

$$\frac{\sqrt{-(di/dt)}}{i} = \frac{1}{zF}\sqrt{\frac{RTV_m}{aV}}(\ln i - \ln A) \qquad (4)$$

where $A = 2FaC_M v \exp(-W/RT)$, $2a$ is the ion jump distance, C_M is the concentration of interstitial ions in the oxide film, v is the ion vibration frequency, W is the activation energy at zero field, z is the ion charge, V is the potential drop in the film, and V_m is the molar volume of the oxide.

The theoretical expression for $(-i')^{1/2}/i$ in the case of the point defect model is presented as [20]:

$$\frac{\sqrt{-(di/dt)}}{i} = \sqrt{\frac{\alpha_2 \varepsilon V_m}{RT}} \qquad (5)$$

where α_2 is the transfer coefficient for the oxygen vacancy generation reaction at the metal/oxide interface, $\varepsilon = V/L$ is the electric field strength in the oxide film, and L is the film thickness.

Examples of the dependence of $F(i) = (-i')^{1/2}/i$ on $\ln i$ are shown in Fig. 6, 7. The derivative at the kth point of the data set was calculated by the formula: $-i'_k = (i_{k-1} - i_{k+1})/(t_{k+1} - t_{k-1})$. As can be seen, in many cases, linear dependence is executed. So, it can be assumed that in these cases, the anodic oxide film grows on the studied silicides in H_2SO_4 solutions by the mechanism of ion migration in a high electric field. In general, linear dependences of $(-i')^{1/2}/i$ on $\ln i$ are well executed for low values of time and correspondingly lesser

thickness of the oxide films. This is in agreement with the general conclusion that the high field model should work better for very thin films [32], because in such films the electric field strength is the highest.

Within the HFM, the expression for the slope of the $\lg i, \lg t$-dependence was obtained [35]:

$$-\frac{d \ln i}{d \ln t} = -\frac{d \lg i}{d \lg t} = \frac{\ln(i/A)}{2 + \ln(i/A)} \qquad (6)$$

The implications of equation (6) are: 1) the slope of $-d\lg i/d\lg t$ is always less than 1 and it can vary over a wide range; 2) the dependence of $\lg i$ on $\lg t$ is not strictly linear, but at significant values of $\ln(i/A)$ and a relatively small time interval the curvature of the chronoamperogram is almost imperceptible. The experimental data (Fig. 1–5, Tables 1, 2) are consistent with (6), at least at low values of t.

The experimental values of the slopes of the dependences of $(-i')^{1/2}/i$ on $\ln i$ are provided in Tables 4, 5. According to (4), the theoretical slope of the dependence of $(-i')^{1/2}/i$ on $\ln i$ within the framework of the HFM is $(1/zF)(RTV_m/aV)^{1/2}$. The values of V_m and a for those oxides which can grow on silicides can only be estimated approximately because: a) the properties of very thin oxide films may differ from those of bulk oxides [19]; b) the exact composition of the oxide film growing on a silicide is not known. There is also an uncertainty regarding the value of V, as the set electrode potential E_f generally does not coincide with the potential drop on the oxide film.

For cobalt oxide CoO, we calculated $V_m = 11.64$ cm³/mol from the molecular weight and density. From the crystallographic data, we obtained the jump distance of the interstitial ions of 0.21 nm. Therefore, the theoretical slope of the dependence of $(-i')^{1/2}/i$ on $\ln i$ for CoO at $V = 1$ V is 8.6 (C/cm²)$^{-1/2}$. For silica, the molar volume is 27.27 cm³/mol [36]. The value of $2a$ is close to the length of the Si–O bond [37], i.e., it is about 0.16 nm. So, the theoretical slope for SiO_2 at $V = 1$ V is 7.53 (C/cm²)$^{-1/2}$ at $z = 4$. Therefore, the theoretical slopes for the considered oxides vary insignificantly, and at V = 1 V they are in the range 7.5–8.6 (C/cm²)$^{-1/2}$. These values are in satisfactory agreement with the results in Tables 4, 5, although in some cases there are noticeable discrepancies. Some of them are
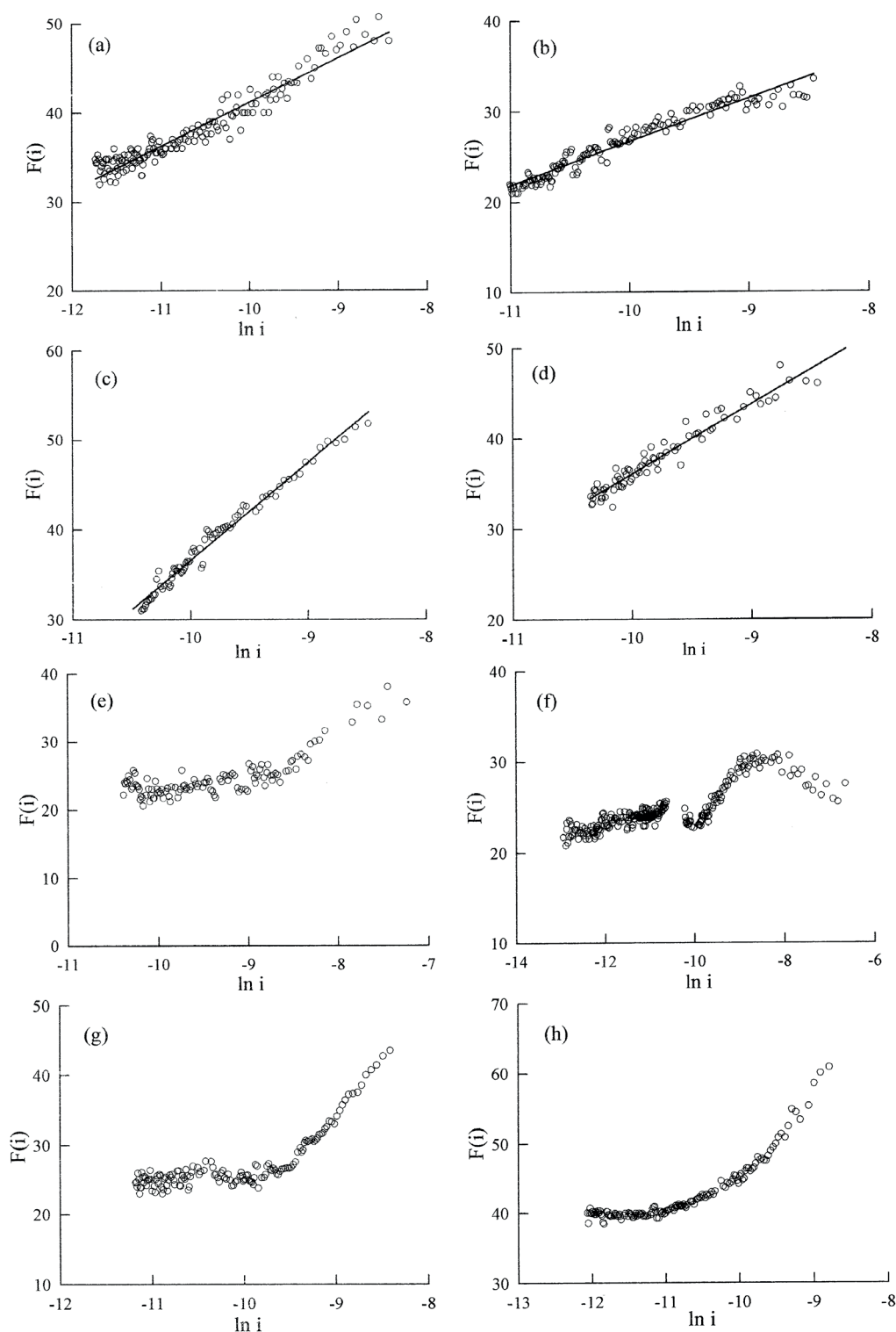
Fig. 6. Dependence of $F(i)$ on $\ln i$ for: a: Co_2Si/0.05 M H_2SO_4, E_f = 1.0 V, the electrode pretreated by mechanical polishing; b: Co_2Si/0.5 M H_2SO_4, E_f = 0.2 V, pretreatment in 2% HF; c: Co_2Si/0.5 M H_2SO_4, E_f = 0.5 V, pretreatment in 2% HF; d: Co_2Si/0.5 M H_2SO_4, E_f = 1.0 V, pretreatment in 2% HF; e: Co_2Si/0.5 M H_2SO_4, E_f = 1.0 V; pretreatment in 2 M KOH; f: Co_2Si/0.5 M H_2SO_4, E_f = 1.0 V; pretreatment in 2 M KOH followed by 30 min at the open circuit potential; g: Co_2Si/0.05 M H_2SO_4, E_f = 1 V; pretreatment in 2 M KOH; and h: Co_2Si/0.5 M H_2SO_4, E = 0.5 V, pretreated by mechanical polishing. The density of the current i is expressed in A/cm², the value of $F(i)$ is in $(C/cm^2)^{-1/2}$
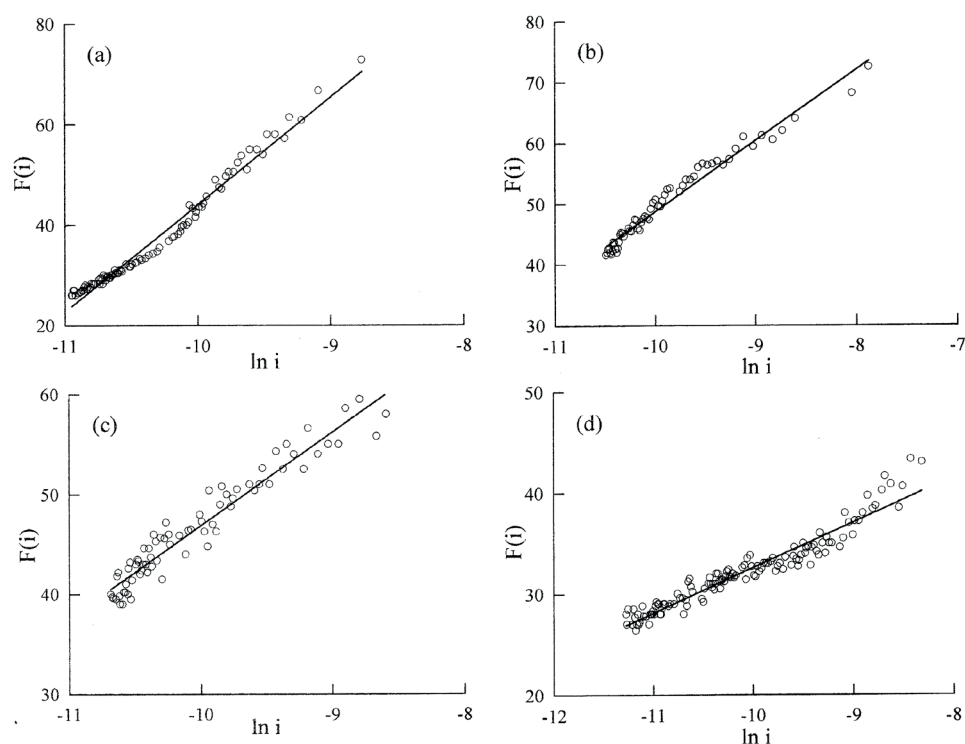
Fig. 7. Dependence of $F(i)$ on $\ln i$ for $CoSi_2/0.5$ M H_2SO_4: a: $E_f = 0.2$ V, pretreatment in 2% HF; b: $E_f = 0.5$ V, pretreatment in 2% HF; c: $E_f = 1.0$ V, pretreatment in 2% HF; and d: $E_f = 1.0$ V, pretreatment in 2 M KOH. The density of the current i is expressed in A/cm^2, the value of $F(i)$ is in $(C/cm^2)^{-1/2}$

Table 4. The values of the slopes of the dependences of $(-di/dt)^{1/2}/i$ on $\ln i$ for the Co_2Si electrode

Pretreatment of electrode surface	Concentration of H_2SO_4, mol L^{-1}	E_f, V	Slope of $(-di/dt)^{1/2}/i$ vs. $\ln i$ plot, $(C\ cm^{-2})^{-1/2}$	Time interval, s
Mechanical polishing	0.05	1.0	5.0	1.5–90
Mechanical polishing	0.5	1.0	5.4	
Mechanical polishing	0.5	0.5	11.5 ~0	0.5–8 > 20
Cathodic polarization	0.5	1.0	6.4	
Treatment in 2% HF	0.5	0.2	6.2	10–100
Treatment in 2% HF	0.5	0.5	10.7	< 20
Treatment in 2% HF	0.5	1.0	6.9	1.2–20
Treatment in 2 M KOH	0.05	1.0	15.0 ~0	1.5–10 > 15
Treatment in 2 M KOH	0.5	1.0	Weak dependence	> 2
Treatment in 2 M KOH, 30 min in 0.5 M H_2SO_4 at E_{oc}	0.5	1.0	Complex weak dependence	

explained by the fact that V is different from 1 V.

The slope $(1/zF)(RTV_m/aV)^{1/2}$ should increase as the potential drop in the oxide film decreases (upon the same electrode pretreatment). This was well achieved for the $CoSi_2$ electrode in 0.5 M H_2SO_4, pretreated in 2% HF. The slope increased from 9.5 to 24.5 as E_f decreased from 1.0 to 0.2 V (Table 5). In the case of the Co_2Si electrode with

the same pretreatment, the slope only increased when E_f decreased from 1.0 V to 0.5 V (Table 4).

For the Co_2Si electrode, the dependences of $(-i')^{1/2}/i$ on $\ln i$ were linear for the mechanically polished electrode or pretreated in 2% HF (Fig. 6a–d). For the Co_2Si electrode pretreated in 2 M KOH solution, when the silicide surface is enriched with cobalt and cobalt oxide may be

Table 5. The values of the slopes of the dependences of $(-di/dt)^{1/2}/i$ on $\ln i$ for the CoSi$_2$ electrode

| Pretreatment of electrode surface	Concentration of H$_2$SO$_4$, mol L^{-1}	E_r, V	Slope of $(-di/dt)^{1/2}/i$ vs. $\ln i$ plot, (C cm^{-2})$^{-1/2}$	Time interval, s
Mechanical polishing	0.5	1.0	21.7	0.6–40
Treatment in 2% HF	0.5	0.2	24.5	0.5–7.5
			14.3	7.5–42
Treatment in 2% HF	0.5	0.5	10.8	0.4–10
Treatment in 2% HF	0.5	1.0	9.55	1.1–19
Treatment in 2% HF	0.05	1.0	19.1	3.5–12
Treatment in 2 M KOH	0.5	1.0	4.5	1–85
Treatment in 2 M KOH	0.5	0.5	8.0	1–48

present on the surface, the value of $(-i')^{1/2}/i$ in a rough approximation does not depend on the current density (Fig. 6e, f). In some cases (Fig. 6g, h), during the growth of the oxide film, there is a transition from a linear change in $F(i)$ with $\ln i$ (in accordance with the HFM) to constant $F(i)$ (in accordance with the PDM). Approximately constant values of $F(i)$ for the Co$_2$Si electrodes pretreated in an alkaline solution are 22–24 (C/cm^2)$^{-1/2}$ at sufficiently large t (Fig. 6e–g). To obtain 22 (C/cm^2)$^{-1/2}$ from relation (5) derived from the PDM, at α_2 = 0.5 and V_m = 11.6 cm^3/mol (as for CoO), the electric field strength in the oxide film must be 2.1·10^5 V/cm, which can be considered a plausible value for the PDM. In contrast to Co$_2$Si, for the CoSi$_2$ electrode, where the oxide is significantly enriched in silicon dioxide [11], the HFM is also achieved upon pretreatment in 2 M KOH (Fig. 7d).

Thus, with a higher cobalt content on the electrode surface (Co$_2$Si silicide with higher volume concentration of cobalt, the Co$_2$Si surface pretreated in a KOH solution), the point defect model is either approximately fulfilled in a wide range of t, or becomes fulfilled at comparatively high t. Under the above conditions, the anodic oxide contains higher amounts of cobalt oxide. The main types of point defects in CoO are cation vacancies [38]. The Co$_3$O$_4$ oxide also contains a stoichiometric excess of oxygen [39]. The formation of point defects in SiO$_2$ is more complicated compared to CoO [40]. These factors contribute to the execution of the PDM for cobalt-rich oxide and do not promote the execution of the PDM for SiO$_2$.

The lg i, lg t-curves with an inflection were observed when using the electrodes pretreated

in 2% HF (Fig. 4, 5). The current density in the lg$i$, lg$t$-dependence section after the inflection were higher compared to the continuation of the initial section into the region of large t. This probably indicates that an additional process is taking place: a) oxidation of cobalt in addition to oxidation of Si resulting in a bilayer structure; b) oxidation of Co(II) to a higher oxidation degree (reaction (3)). The higher current densities in 0.05 M H$_2$SO$_4$ (Fig. 4, 5) can be explained by the fact that with an increase in pH, the equilibrium potential of oxidation reactions (1)–(3) shifts in the negative direction. That is, at a given E_r, a higher anodic overpotential is generated, which provides an increase in i at the beginning of passivation.

For Co$_2$Si pretreated in 2% HF, the dependences $F(i)$ on $\ln i$ for the whole studied interval of t (up to 3000 s) have a complex shape (Fig. 8): at low t
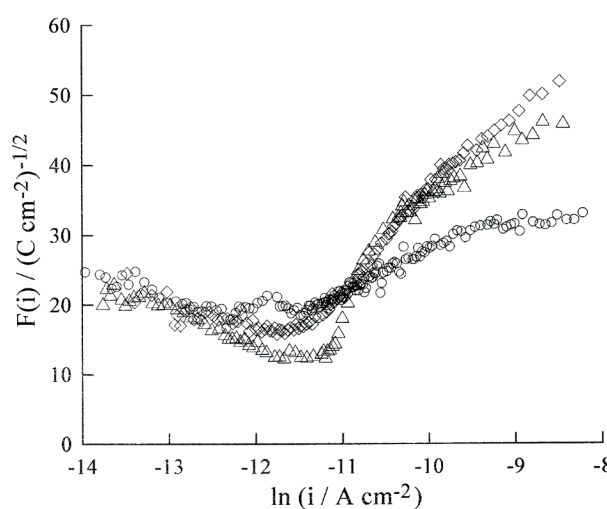
Fig. 8. Chronoamperograms for Co$_2$Si/0.5 M H$_2$SO$_4$ over a wide time interval, pretreatment in 2% HF. Potential E_r, V: (◯) – 0.2; (◇) – 0.5; (△) – 1.0

(large i) there is a linear section, then there is a minimum (corresponds to the inflection on the lg$i$,lg$t$-curves), and then $F(i)$ becomes almost the same constant value for all E_f. The constant value of $F(i)$ at large t could indicate that the point defect model is executed. At high t (relatively thick oxide films), $F(i)$ has the same value of 22–24 (C/cm^2)$^{-1/2}$ as after pretreatment in a solution of 2 M KOH. Apparently, when thicker films are formed, the oxide is gradually enriched with cobalt also when the electrode is pretreated in 2% HF or two-layer structures are formed. The structures consist of a SiO$_2$ layer and a layer enriched with cobalt oxide under it.

4. Conclusions

The study showed that the kinetics of the anodic oxide film growth on cobalt silicide in sulphuric acid solutions significantly depends on the pretreatment of the electrode surface. This agrees with the literature data indicating that the presence of the native oxide film and surface pretreatment are important factors influencing the formation of the passive films [41, 42].

It was shown that a large number of results are adequately described by the high field model. This is particularly true for the data obtained at short passivation time (up to 30–50 s) without the pretreatment of the Co$_2$Si electrode in an alkaline solution. When the silicide surface is enriched with metal (Co$_2$Si pretreated in a 2 M KOH solution) before passivation, the point defect model is executed with sufficiently high values of time.

Author contributions

All authors made an equivalent contribution to the preparation of the publication.

Conflicts of interest

The authors declare that they have no known competing financial interests or personal relationships that could have influenced the work reported in this paper.

References

1. Maurice V., Marcus P. Current developments of nanoscale insight into corrosion protection by passive oxide films. *Current Opinion in Solid State and Materials Science*. 2018;22(4): 156–167. https://doi.org/10.1016/j.cossms.2018.05.004

2. Shein A. B. *Electrochemistry of silicides and germanides of transition metal**. Perm: Perm State Univ. Publ., 2009. 269 p. (In Russ)

3. Schmidt C., Strehblow H.-H. The passivity of Fe/Si alloys in aqueous electrolytes at pH 5 and 9 studied by X-ray photoelectron spectroscopy and ion scattering spectroscopy. *Journal of the Electrochemical Society*. 1998;145(3): 834–840. https://doi.org/10.1149/1.1838353

4. Strehblow H.-H., Maurice V., Marcus P. Passivity of metals. In: *Corrosion Mechanisms in Theory and Practice*. P. Marcus (ed.). CRC Press, Taylor & Francis Group; 2012. pp. 235–326.

5. Wolff U., Schneider F., Mummert K., Schultz L. Stability and electrochemical properties of passive layers on Fe-Si alloys. *Corrosion*. 2000;56(12): 1195–1201. https://doi.org/10.5006/1.3280507

6. Chen H., Ma Q., Shao X., Ma J., Huang B. X. Corrosion and microstructure of the metal silicide (Mo$_{1-x}$Nb$_x$)$_5$Si$_3$. *Corrosion Science*. 2013;70: 152–160. https://doi.org/10.1016/j.corsci.2013.01.024

7. Tang C., Wen F., Chen H., Liu J., Tao G., Xu N., Xue J. Corrosion characteristics of Fe$_3$Si intermetallic coatings prepared by molten salt infiltration in sulfuric acid solution. *Journal of Alloys and Compounds*. 2019;778: 972–981. https://doi.org/10.1016/j.jallcom.2018.11.198

8. Hu L., Hu B., Gui, Y. Study on the melting and corrosion resistance of Fe-Cr-Si dual phase alloy. *IOP Conference Series: Materials Science and Engineering*. 2020;782(2): 022031. https://doi.org/10.1088/1757-899X/782/2/022031

9. Zhang Y., Xiao J., Zhang Y., Liu W., Pei W., Zhao A., Zhang W., Zeng, L. The study on corrosion behavior and corrosion resistance of ultralow carbon high silicon iron-based alloy. *Materials Research Express*. 2021;8(2): 026504. https://doi.org/10.1088/2053-1591/abdc52

10. Shadrin K. V., Panteleeva V. V., Shein A. B. Passivation of chromium dicilicide in acidic media. *Bulletin of Perm University. Chemistry*. 2021;11(3): 202–211 (In Russ., abstract in Eng.). https://doi.org/10.17072/2223-1838-2021-3-202-211

11. Baklanov M. R., Badmaeva I. A., Donaton R. A., Sveshnikova L. L., Storm W., Maex K. Kinetics and mechanism of the etching of CoSi$_2$ in HF-based solutions. *Journal of the Electrochemical Society*. 1996;143(10): 3245–3251. https://doi.org/10.1149/1.1837192

12. Strehblow H.-H. Passivity of metals. In: *Advances in Electrochemical Science and Engineering. Vol. 8*. R. C. Alkire (ed.). Wiley; 2002. pp. 271–374. https://doi.org/10.1002/3527600787.ch4

13. Panteleeva V. V., Shein A. B. Growth of anodic oxide films on iron-triad metal monosilicides in sulfuric acid electrolyte. *Russian Journal of*

Electrochemistry. 2014;50(11): 1036–1043. https://doi.org/10.1134/S102319351411007X

14. Behazin M., Biesinger M. C., Noël J. J., Wren J. C. Comparative study of film formation on high-purity Co and Stellite-6: Probing the roles of a chromium oxide layer and gamma-radiation. *Corrosion Science.* 2012;63: 40–50. https://doi.org/10.1016/j.corsci.2012.05.007

15. Lutton K., Gusieva K., Ott N., Birbilis N., Scully J. R. Understanding multi-element alloy passivation in acidic solutions using operando methods. *Electrochemistry Communications.* 2017;80: 44–47. https://doi.org/10.1016/j.elecom.2017.05.015

16. Lutton Cwalina K., Ha H. M., Ott N., Reinke P., Birbilis N., Scully J. R. In operando analysis of passive film growth on Ni-Cr and Ni-Cr-Mo alloys in chloride solutions. *Journal of the Electrochemical Society.* 2019;166(11): C3241–C3253. https://doi.org/10.1149/2.0261911jes

17. Wang Z., Di-Franco F., Seyeux A., Zanna S., Maurice V., Marcus P. Passivation-induced physicochemical alterations of the native surface oxide film on 316L austenitic stainless steel. *Journal of the Electrochemical Society.* 2019;166(11): C3376–C3388. https://doi.org/10.1149/2.0321911jes

18. Choudhary S., Thomas S., Macdonald D. D., Birbilis N. Growth kinetics of multi-oxide passive film formed upon the multi-principal element alloy AlTiVCr: Effect of transpassive dissolution of V and Cr. *Journal of the Electrochemical Society.* 2021;168: 051506. https://doi.org/10.1149/1945-7111/ac0018

19. Burstein G. T. Passivity and localized corrosion. In: *Corrosion. Vol. 1. Metal/Environment Reactions.* L. L. Shreir, R. A. Jarman, G. T. Burstein (eds.). Oxford: Butterworth-Heinemann; 1994. pp. 1:118–1:150. https://doi.org/10.1016/b978-0-08-052351-4.50013-3

20. Zhang L., Macdonald D. D., Sikora E., Sikora J. On the kinetics of growth of anodic oxide films. *Journal of the Electrochemical Society.* 1998;145(3): 898–905. https://doi.org/10.1149/1.1838364

21. Kichigin V. I., Shein A. B. Effect of anodising on the kinetics of the hydrogen evolution reaction on cobalt silicides in sulphuric acid solution. *Condensed Matter and Interphases.* 2017;19(3): 359–367 (In Russ., abstract in Eng.). https://doi.org/10.17308/kcmf.2017.19/212

22. Liu D. Q., Blackwood D. J. Mechanism and dissolution rates of anodic oxide films on silicon. *Electrochimica Acta.* 2013;105: 209–217. https://doi.org/10.1016/j.electacta.2013.04.024

23. Thissen P., Seitz O., Chabal Y. J. Wet chemical surface functionalization of oxide-free silicon. *Progress in Surface Science.* 2012;87(9-11): 272–290. https://doi.org/10.1016/j.progsurf.2012.10.003

24. Seidel H., Csepregi L., Heuberger A., Baumgärtel H. Anisotropic etching of crystalline silicon in alkaline solutions. I. Orientation dependence and behavior of passivation layers. *Journal of the Electrochemical Society.* 1990;137(11): 3612–3626. https://doi.org/10.1149/1.2086277

25. Kichigin V. I., Shein A.B . Anodic behavior of Co_2Si in potassium hydroxide solutions. *Bulletin of Perm University. Chemistry.* 2011;1(3): 4–14 (In Russ., abstract in Eng.). Available at: https://www.elibrary.ru/download/elibrary_17563295_89020211.pdf

26. Sukhotin A. M. (ed.). *Handbook of Electrochemistry*.* Leningrad: Khimiya Publ.; 1981. 488 p. (In Russ.).

27. Lohrengel M. M. Thin anodic oxide layers on aluminium and other valve metals: high field regime. *Materials Science and Engineering: R: Reports.* 1993;11(6): 243–294. https://doi.org/10.1016/0927-796X(93)90005-N

28. Vanhumbeeck J. F., Proost J. Current understanding of Ti anodisation: fundamental, morphological, chemical and mechanical aspects. *Corrosion Reviews.* 2009;27: 117–204. https://doi.org/10.1515/CORRREV.2009.27.3.117

29. Macdonald D. D. The point defect model for the passive state. *Journal of the Electrochemical Society.* 1992;139(12): 3434–3449. https://doi.org/10.1149/1.2069096

30. Roh B., Macdonald D. D. Passivity of titanium: part II, the defect structure of the anodic oxide film. *Journal of Solid State Electrochemistry.* 2019;23: 1967–1979. https://doi.org/10.1007/s10008-019-04254-0

31. Bösing I., La Mantia F., Thöming J. Modeling of electrochemical oxide film growth – a PDM refinement. *Electrochimica Acta.* 2022;406: 139847. https://doi.org/10.1016/j.electacta.2022.139847

32. Seyeux A., Maurice V., Marcus P. Oxide film growth kinetics on metals and alloys. I. Physical model. *Journal of the Electrochemical Society.* 2013;160(6): C189–C196. https://doi.org/10.1149/2.036306jes

33. Momeni M., Behazin M., Wren J. C. Mass and charge balance (MCB) model simulations of current, oxide growth and dissolution during corrosion of Co-Cr alloy Stellite-6. *Journal of the Electrochemical Society.* 2016;163(3): C94–C105. https://doi.org/10.1149/2.0721603jes

34. Lutton K., Scully J. R. Kinetics of oxide growth of passive films on transition metals. *Encyclopedia of Interfacial Chemistry, Surface Science and Electrochemistry.* 2018;284–290. https://doi.org/10.1016/B978-0-12-409547-2.13576-0

35. Burstein G. T., Davenport A. J. The current-time relationship during anodic oxide film growth under high electric field. *Journal of the Electrochemical Society.* 1989;136(4): 936–941. https://doi.org/10.1149/1.2096890

36. Franssila S. *Introduction to Microfabrication.* John Wiley & Sons; 2010. 518 p. https://doi.org/10.1002/9781119990413

37. Nascimento M. L. F., Zanotto E. D. Diffusion processes in vitreous silica revisited. *Physics and Chemistry of Glasses - European Journal of Glass Science and Technology Part B*. 2007;48(4): 201–217. Available at: https://www.ingentaconnect.com/contentone/sgt/ejgst/2007/00000048/00000004/art00001

38. Koel G. J., Gellings P. J. The contribution of different types of point defects to diffusion in CoO and NiO during oxidation of the metals. *Oxidation of Metals*. 1972;5: 185–203. https://doi.org/10.1007/BF00609658

39. Razina N. F. *Oxide electrodes in aqueous aolutions**. Alma-Ata: Nauka Publ.; 1982. (In Russ.).

40. Deml A. M., Holder A. M., O'Hayre R. P., Musgrave C. B. Intrinsic material properties dictating oxygen vacancy formation energetics in metal oxides. *The Journal of Physical Chemistry Letters*. 2015;6(10): 1948–1953. https://doi.org/10.1021/acs.jpclett.5b00710

41. Vargas R., Carvajal D., Galavis B., Maimone A., Madriz L., Scharifker B. R. High-field growth of semiconducting anodic oxide films on metal surfaces for photocatalytic application. *International Journal of Photoenergy*. 2019: 2571906. https://doi.org/10.1155/2019/2571906

42. Ma L., Pascalidou E.-M., Wiame F., Zanna S., Maurice V., Marcus P. Passivation mechanisms and pre-oxidation effects on model surfaces of FeCrNi austenitic stainless steel. *Corrosion Science*. 2020;167; 108483. https://doi.org/10.1016/j.corsci.2020.108483

* Translated by author of the article.

Information about the authors

Anatoliy B. Shein, Dr. Sci. (Chem.), Full Professor, the Department of Physical Chemistry, Perm State University (Perm, Russian Federation).

https://orcid.org/0000-0002-2102-0436

ashein@psu.ru

Vladimir I. Kichigin, Cand. Sci. (Chem.), Research Fellow at the Department of Physical Chemistry, Perm State University (Perm, Russian Federation).

https://orcid.org/0000-0002-4668-0756

kichigin@psu.ru

Translated by Anastasiia Ananeva
Edited and proofread by Simon Cox